The Journal of Physical Chemistry A

 VOLUME 103, NUMBER 35, SEPTEMBER 2, 1999

LETTERS

Dissociative Electron Attachment during the Laser Desorption of Anthracene Picrate

Steven M. Hankin and Phillip John*

Department of Chemistry, Heriot-Watt University, Riccarton, Edinburgh, EH14 4AS, UK

Received: May 25, 1999; In Final Form: July 14, 1999

The laser desorption of the charge-transfer complex anthracene−picrate has been studied by post-ionization time-of-flight (L2ToF) mass spectrometry. Mass spectra recorded after post-ionization of the desorbed plume exhibited negative-ion signals exclusively associated with picric acid. Furthermore, these negative ions were observed only as the focus of the ionization laser beam was moved to within 150 μm of the point of desorption. Negative ions were not present in the L2ToF mass spectra of picric acid alone but were observed only in the presence of anthracene. While the charge-transfer complex is not expected to remain intact following laser desorption into the gas phase, the generation of negative ions upon laser irradiation of the desorbed plume occurs through interaction of the neutral picric acid molecules with electrons produced by in-situ photoionization of the anthracene component. Acceleration of the primary electrons through the high-density plume induces electron attachment and subsequent fragmentation of picric acid. The spatial profile of the ions created in the plume arising from the laser desorption of anthracene picrate supports a PAH-mediated electron attachment phenomenon leading to the formation of negatively charged ions.

Introduction

Polycyclic aromatic hydrocarbons (PAHs) are known to form complexes with a variety of acceptor molecules including aromatic amines,[1−3] nitrobenzene derivatives,[4−7] and cyclodextrins.[8] As part of a L2ToF mass spectrometric investigation of weakly bound molecular complexes, we have studied the laser desorption of the archetypal charge-transfer complex formed between anthracene and picric acid (2,4,6-trinitrophenol). Charge-transfer complexes formed between PAHs and picric acid have been studied by spatially resolved laser time-of-flight mass spectrometry.[9]

Laser desorption/post-ionization time-of-flight mass spectrometry[10−12] (L2ToFMS) has become an established analytical tool for the study of organic[13−20] and inorganic materials.[21−23] The essence of the L2ToFMS technique is that a plume of neutral molecules is created on irradiation of a solid sample with a pulsed UV or IR desorption laser. Ions are created in the desorbed plume with a second time-delayed nanosecond or femtosecond laser pulse and subsequently analyzed by time-of-flight mass spectrometry. A number of advantages can be delineated from the development of L2ToFMS. First, spatially and temporarily decoupling the desorption from the ionization process allows lower desorption powers to be used, reducing the degree of molecular dissociation or fragmentation. Second, the ionization laser power can be varied independently to yield mass spectra, in the case of PAHs, dominated by the parent ion. Third, the ability to position the focus of the post-ionization laser beam to ∼50 μm from the sample surface has provided an insight to the phenomena occurring in the high-density regions of the desorption plume. The observation of negative ions has previously been reported for single-step laser ionization experiments.[24] Although the formation of ions in a single-step process is more complex than discrete gas-phase photoionization (as in L2ToFMS), the origin of the negative ions

* Corresponding author. E-mail: P.John@hw.ac.uk. Fax: +44 (0)131 451 3180.

10.1021/jp991702h CCC: $18.00
Published on Web 08/14/1999

within the laser-desorbed plume was suggested to be a result of electron collisions with neutral molecules.

We report on the observation of gas-phase generation of negative ions from the laser irradiation of a desorbed plume of anthracene picrate using L2ToFMS. Moreover, the spatial dependence of the phenomenon supports an electron attachment process occurring within the laser-desorbed plume.

Experimental Section

The laser desorption/post-ionization time-of-flight mass spectrometer has been described in previous publications.[9,25] Achromatic focusing of the 266 nm Nd:YAG (Quanta-Ray DCR-11, Spectra Physics) laser pulse normal to the sample surface was accomplished using a Cassegrain objective (focal length = 14 mm) achieving typical diameters at the focus in the range of 1−2 μm. At 1 Hz the desorption laser power density was maintained at ca. 15 MW cm^{-2} (∼20 nJ per pulse). The desorbed neutrals were ionized at 266 nm using a second Nd:YAG laser (Quanta-Ray DCR-11, Spectra-Physics) at an energy of <10 μJ per pulse. The focus of the ionization laser beam was located ∼40 μm above the sample surface. The beam was focused into the center of the ablation plume using a fused silica UV-grade plano-convex lens (focal length = 150 mm, diameter = 25 mm). Synchronous firing of the two Nd:YAG lasers was controlled using a variable time delay unit (0−50 ms, 20 ns jitter). The post ionization signal was contingent on the presence of both laser pulses; removal of either eliminated the signal. The ions were accelerated using an Einzel lens located ca. 4 mm in front of the sample surface. The ions were mass separated using a 2 m long flight tube fitted with a reflectron. The ions were detected by a dual microchannel plate (Galileo 3025MA) detector, and the amplified signal was fed to a 175 MHz transient digitizer (LeCroy 9400A). The digitized data were transferred to a PC and analyzed using proprietary software (Grams 32, Galactic).

Equimolar (0.28 M) solutions (2 mL) of anthracene (Aldrich, 98% purity) and picric acid (Aldrich, 98% purity) were prepared using HPLC grade toluene (Aldrich). Slow evaporation of the supernatant liquor under ambient conditions yielded large red crystals of anthracene picrate which were removed and placed onto an aluminum stub for L2ToFMS analysis at room temperature. Mixtures of graphite (20% suspension of submicron particles in propanol, David Hart Ltd) or 2,5-dihydroxybenzene (Aldrich, 98% purity; 0.2 M in methanol) with picric acid were prepared by co-depositing 0.1 mL of the graphite suspension or 2,5-DHB with 0.2 mL of the above-mentioned picric acid solution onto an aluminum stub. Upon evaporation of the solvent, yellow picric acid microcrystallites were observed to be coated with graphite or 2,5-DHB.

Results

The positive ion L2ToF mass spectra of anthracene picrate at room temperature exhibited the molecular ion of anthracene at 178 Da as shown in the upper trace of Figure 1. The parent-ion envelope was identical to that observed for pure anthracene, comprising $[M\text{-}nH]^+$ peaks where $n = 1-4$ and the $[M + 1]^+$ ion at 179 Da. The ratio of the ^{13}C isotopomer and parent-ion peak areas was in agreement with the calculated natural abundance ratio (13.4%) confirming that anthracene did not undergo protonation by picric acid. At powers <15 MW cm^{-2}, ion signals were not observed when only the desorption laser pulse was fired on the sample. Despite a thorough search, the parent ion of anthracene picrate was not observed.

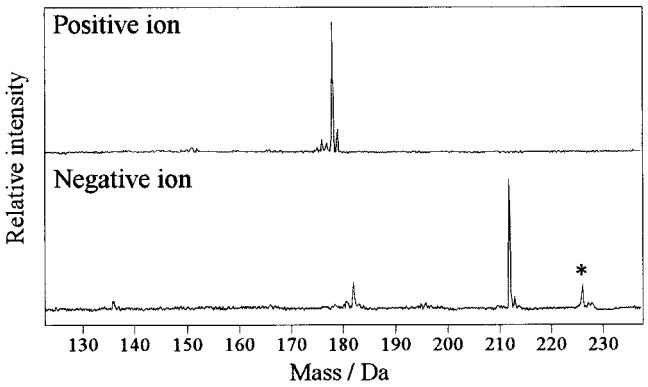

Figure 1. L2ToF mass spectra of anthracene picrate. Positive-ion mass spectrum (upper trace) exhibits the anthracene parent-ion envelope. Negative-ion mass spectrum (lower trace) exhibits picric acid fragments only. The peak marked with an asterisk arises from the single-laser ionization of the solid.

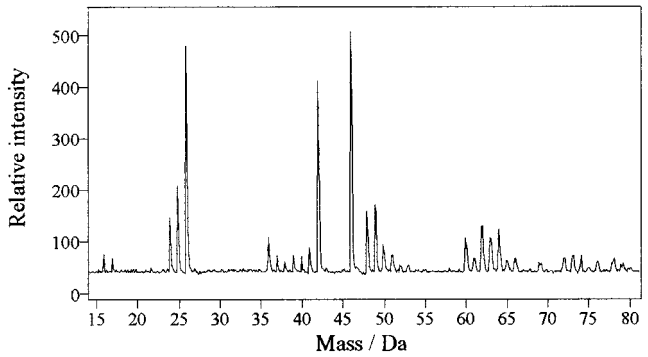

Figure 2. Negative-ion L2ToF mass spectrum of anthracene picrate exhibiting low-mass fragments.

The corresponding negative-ion mass spectrum is shown in the lower trace of Figure 1. In the absence of the ionization laser pulse, a weak ion signal was observed. This ion signal was assigned as $[P-H]^-$ and originated from the single-laser desorption/ionization of the picrate component of the complex. Upon irradiating the plume with the post-ionization laser pulse, the mass spectra exhibited peaks at 136, 182, 196, 212, and a minor peak at 228 Da. Fragmentation of the picric acid moiety (P, 229 Da) yielded $[P-OH-NO-NO_2]^-$, $[P-OH-NO]^-$, $[P-OH-O]^-$, $[P-OH]^-$, and $[P-H]^-$. The most intense peak was observed at 212 Da corresponding to $[P-OH]^-$. Low-mass fragment ions were also observed as shown in Figure 2. These were $[H]^-$, $[O]^-$, $[OH]^-$, $[C_nH_y]^-$ carbon clusters where $n = 2-6$ and $y = 0-5$, and intense negative ion signals at 26, 42, and 46 Da assigned to $[CN]^-$, $[CNO]^-$, and $[NO_2]^-$, respectively. Signals corresponding to $[NO]^-$ were not observed in any of the mass spectra. L2ToF analysis of picric acid alone did not give rise to negative-ion signals even when mixed with graphite or 2,5-DHB, commonly used additives that have been used to enhance the desorption yield of neutral molecules from solid samples.

Spatial probing of the neutral desorbed plume was performed at a fixed desorption power density of 15 MW cm^{-2}. The anthracene positive-ion signal at 178 Da $[anthracene]^+$ and the picric acid fragment ion at 212 Da $[P-OH]^-$ were determined as a function of distance from the substrate at a fixed delay time of 0.5 μs between the desorption and post-ionization laser pulses. The two spatial distributions are compared in Figure 3. Only the relative positive- and negative-ion signal intensities are illustrated since the detector response for positive and negative ions differs and the spectra were obtained at slightly

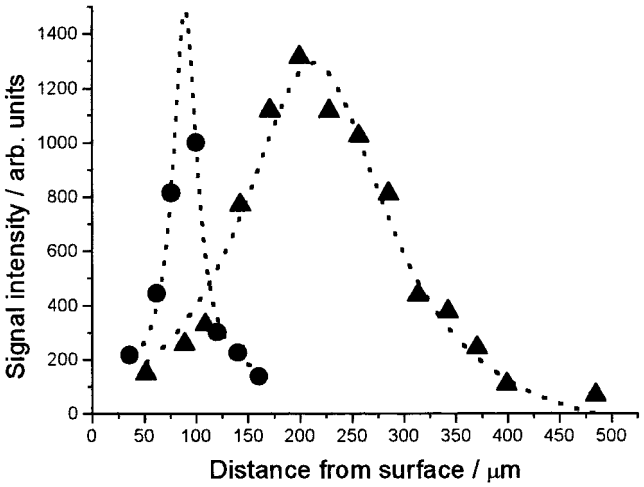

Figure 3. Dependence of the ion signals for $[anthracene]^+$ (▲) and $[picric\ acid-OH]^-$ (●) on the distance of the ionization laser focus from the substrate. The curves are included as a guide to the eye.

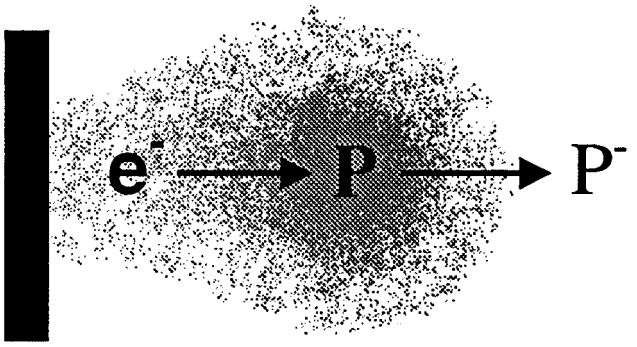

Figure 4. Schematic illustration of PAH-mediated electron-capture phenomenon. Electrons produced by photo-ionization of anthracene are accelerated into the high-density region of the plume creating energized negative ions which subsequently fragment.

different ion extraction voltages. The two profiles clearly illustrate that the maximum signal intensities of the positive- and negative-ion signals occur at different distances from the substrate. Figure 3 shows that the peak of the negative-ion distribution was observed to be ~100 μm closer to the surface than the positive-ion distribution. The error in the position was estimated to be ±15 μm and the data points represent the signal intensity averaged over 50 laser shots.

Discussion

The laser desorption of anthracene picrate at 266 nm, in principle, could lead to the presence of the molecular complex $[A^{\delta+}\cdot P^{\delta-}]$, free anthracene [A], and picric acid [P] in the laser-generated plume. The absorption characteristics of the solid matrix is affected by the presence of anthracene. The absorption maxima observed in the spectra of the donor and acceptor components are barely altered on complexation.[6] Thus the absorption of the charge-transfer complex will be dominated by the PAH which exhibits the more intense absorption band at 266 nm. Hence, the desorption of picric acid into the gas phase may be greatly enhanced by the increased absorption properties of the sample, as anthracene exhibits a near resonance ($S_3 \leftarrow S_0$) absorption at 252 nm.[26] The absence of post-ionization signals in the mass spectra of a mixture of picric acid with graphite powder or 2,5-DHB eliminates the direct ionization of picric acid in the plume as a channel for negative ion production. The latter materials strongly enhance the absorption properties of the sample, leading to a significant increase in the desorption yield[27] with no evidence of photo-ionization in the plume.

The presence of only a minor negative-ion signal upon firing the desorption laser alone suggests that immediate dissociation and fragmentation of the complex during desorption is not a significant ion channel. However, anthracene−picrate has a binding energy[26] of less than 0.2 eV suggesting that an intact complex is unlikely to survive laser desorption at 266 nm ($h\nu$ = 4.66 eV). L2ToF mass spectra revealed that laser irradiation of the desorbed plume arising from the anthracene/picric acid complex gave rise to positive ions of anthracene and negative ions derived from picric acid. Maintaining the desorption laser power below the threshold for single-laser ionization ensured that the desorbed plume comprised neutral species.

The relative positions for the positive- and negative-ion signal maxima are shown in Figure 3. The maximum density of neutral molecules in the plume was located using the signal maxima of the post-ionization of anthracene. The signal maximum for $[anthracene]^+$ was observed to be ~200 μm from the surface, whereas the negative-ion signal maximum for $[P-OH]^-$ was observed to be ~100 μm from the surface, approximately midway between the surface and the maximum neutral molecule density of the plume. The appearance of the negative-ion maximum displaced from the anthracene maximum is a significant finding in terms of the reactions occurring in the desorbed plume. Since negative-ion signals were observed only in the presence of the ionization laser pulse, processes induced by the emission of electrons from the sample surface can be ruled out.

The observed negative-ion fragments were associated with the loss of O, OH, NO, and NO_2 groups from the picric acid. Electron-capture negative-ion mass spectrometry has been employed to elucidate the mechanism of the fragmentation of 2,4-dinitrophenol among other nitro compounds.[28] The 2,4-dinitrophenol derivatives show molecular ions, $[M\text{-}OH]^-$ ions, $[M\text{-}NO]^-$ ions, and $[M\text{-}OH-NO]^-$ ions. The highest-intensity peak was the $[M\text{-}OH]^-$ ion. The relative intensities are very similar to those observed in the present work. In the L2ToFMS of anthracene picrate, the loss of NO and NO_2 from the parent molecules of picric acid is similar to that observed during the laser ionization of 9-nitroanthracene and 1-nitropyrene.[24]

Gas-phase anthracene ionizes readily via a two-photon ionization process[26] that is easily accessible using 266 nm laser radiation. The electrons arising from the two-photon ionization of anthracene are produced in an electric field gradient and are accelerated to energies commensurate with dissociative electron attachment.[29] While there is no evidence for electron attachment to anthracene itself during plume expansion, we propose that the presence of negative ions in the plume arises from electron attachment to picric acid.

Inspection of Figure 3 shows that the negative-ion signal maximum occurs at a position ~100 μm *before* the maximum neutral density of the plume. The spatial separation of positive- and negative-ion signals is accounted for by the following mechanism. In the absence of electron-capture data for picric acid, we base our arguments on the data for nitroaromatics.[30,31] A series of resonances for electron capture are observed for the production of the molecular and fragment ions. For example, three distinct negative ion resonances for the molecular radical anion of nitrobenzene[31] have been reported at energies of 0.06, 3.3 and 6.9 eV. More recent high-resolution data[32] shows that resonances at 3.3, and 6.9 eV result in the production of $[M-H]^-$, not $[M]^{\bullet-}$. The energy of the electrons ejected from the two-photon ionization of anthracene is ~1.9 eV, based on

the IP of anthracene[33] being 7.4 eV and the $2h\nu$ (266 nm) being 9.32 eV. Therefore, the nascent electron energy precludes the formation of negative ions from near-zero energy resonances. Higher-energy resonances may be accessed through the capture of electrons which have been accelerated by the field.

The electric field contours of the source were calculated by a 2D simulation using the SIMION 3D v.6 ion trajectory software. These calculations show that the field gradient is linear from the substrate to a distance of ~2.5 mm. In this region, which includes the ionization focus, the field gradient is 0.34 V μm^{-1}. Close to the substrate (<50 μm), the electron density is necessarily low because of the low neutral density of the plume. Electrons from a location of 25 μm acquire an energy of ~59 eV before encountering the highest-density region of the plume. The contribution of these two effects leads to a low ion yield. At greater distances from the surface (>175 μm) the electron density is larger but the energy acquired from the field (<17 eV) is insufficient for dissociative electron attachment. Therefore the negative-ion yield curve shows a narrow distribution. As a corollary, the electrons must pass through the highest-density part of the plume. Otherwise, the negative-ion distribution would be broader than the positive-ion spatial distribution as a result of electrons generated at distances greater than 300 μm interacting with the dilute portion of the leading edge of the plume.

The mass resolution observed in negative-ion spectra was significantly lower (~200) than the positive-ion spectra (~600). This suggests that the negative ions are generated over a longer time period compared to PAH positive ions. This is indicative of electron attachment reactions[34] occurring in the plume rather than a photo-ionization process occurring at the laser focus.

Further support for the proposed mechanism arises from consideration of the electron affinity (EA) and electron capture rate constants of the reacting species. The electron affinity[35] of anthracene and *m*-nitrotoluene are 0.60 and 0.99 eV, respectively. The electron-capture rate constants for gas-phase anthracene[36,37] and *m*-nitrotoluene[30] at room temperature have been reported as 1×10^{-9} and 0.25×10^{-7} cm^3 s^{-1}, respectively. It is apparent from these data that electron capture by the nitroaromatic component of the plume is expected to dominate. The electron-capture rate constants for other PAHs and nitrobenzene derivatives have also been determined in these works, although it has been suggested that considerable differences in the molecular structure of molecules will mask the subtle effect that changes in the electron affinity have on the overall rate constant for electron attachment.

Although the predicted electron energies in the present work are greater than those employed in conventional electron attachment experiments, it is not inconceivable that the positive ions and the high density of neutral molecules may alter the kinetic energy distribution of the electrons through space−charge interactions and collisions in the plume. Due to the high-density nature of the plume, the possibility of other ion−molecule or third body reactions cannot be excluded.

In summary, techniques capable of probing within micrometers of the sample surface offer an insight into the processes occurring in the early stages of plume development. This work has exemplified the complex behavior occurring in the high-density region of laser-desorbed plumes when in the presence of large electric-field gradients. Furthermore, we have demonstrated the potential use of laser desorption and photo-ionization for dissociative electron attachment studies of involatile substances exhibiting high electron-capture cross sections.

Acknowledgment. We acknowledge Heriot-Watt University for a scholarship (S.M.H.) and Edinburgh Surface Analysis Technology for further support. We thank Dr. I. C. Walker for valuable advice on electron attachment processes.

References and Notes

(1) Brenner, V.; Millié, Ph.; Piuzzi, F.; Tramer, A. *J. Chem. Soc., Faraday Trans.* **1997**, *93*, 3277.

(2) Tramer, A.; Brenner, V.; Millié, Ph.; Piuzzi, F. *J. Phys. Chem. A* **1998**, *102*, 2798.

(3) Tramer, A.; Brenner, V.; Millié, Ph.; Piuzzi, F. *J. Phys. Chem. A* **1998**, *102*, 2808.

(4) Sudborough, J. J. *J. Chem. Soc.* **1916**, *109*, 1339.

(5) Dewar, M. J. S.; Lepley, A. R. *J. Am. Chem. Soc.* **1961**, *83*, 4560.

(6) Tombesi, O. L.; Frontera, M. A.; Tomas, M. A.; Badajoz, M. A. *Appl. Spectrosc.* **1992**, *46*, 873.

(7) Reshamwala, I. H. *Pakistan J. Sci. Ind. Res.* **1966**, *9*, 203.

(8) Blyshak, L. A.; Dodson, K. Y.; Patonay, G.; Warner, I. M.; May, W. E. *Anal. Chem.* **1989**, *61*, 955.

(9) Hankin, S. M.; John, P.; Smith, G. P. *Anal. Chem.* **1997**, *69*, 2927.

(10) *Lasers in Mass Spectrometry*; Lubman, D. M., Ed.; Oxford University Press: Oxford, 1990.

(11) *Laser Ionization Mass Analysis*; Vertes, A., Gijbels, R., Adams, F., Eds.; Wiley-Interscience: New York, 1993.

(12) Houk, R. S. In *Analytical Applications of Lasers*; Piepmeier, E. H., Ed.; Wiley-Interscience: New York, 1986.

(13) De Vries, M. S.; Elloway, D. J.; Wendt, H. R.; Hunziker, H. E. *Rev. Sci. Instrum.* **1992**, *63*, 3321.

(14) Schilke, D. M.; Levis, R. J. *Rev. Sci. Instrum.* **1994**, *65*, 1903.

(15) Voumard, P.; Zhan, Q.; Zenobi, R. *Rev. Sci. Instrum.* **1993**, *64*, 2215.

(16) Lykke, K. R.; Wurz, P.; Parker, D. H.; Pellin, M. J. *Appl. Optics* **1993**, *32*, 857.

(17) Kovalenko, L. J.; Maechling, C. R.; Clemett, S. J.; Philippoz, J.-M.; Zare, R. N.; Alexander, C. M. O. *Anal. Chem.* **1992**, *64*, 682.

(18) Dale, M. J.; Jones, A. C.; Pollard, S. J. T.; Langridge-Smith, P. R. R. *Analyst* **1994**, *119*, 571.

(19) Zenobi, R. *Chimia* **1994**, *48*, 64.

(20) Haefliger, O. P.; Zenobi, R. *Anal. Chem.* **1998**, *70*, 2660.

(21) Ma, Z.; Thompson, R. N.; Lykke, K. R.; Pellin, M. J.; Davis, A. M. *Rev. Sci. Instrum.* **1995**, *66*, 3168.

(22) Nicolussi, G. K.; Pellin, M. J.; Lykke, K. R.; Trevor, J. L.; Mencer, D. E.; Davis, A. M. *Surf. Interface Anal.* **1996**, *24*, 363.

(23) Savina, M. R.; Lykke, K. R. *Anal. Chem.* **1997**, *69*, 3741.

(24) Bezabeh, D. Z.; Allen, T. M.; McCauley, E. M.; Kelly, P. B.; Jones, A. D. *J. Am. Soc. Mass Spectrom.* **1997**, *8*, 630.

(25) Hankin, S. M.; John, P.; Simpson, A. W.; Smith, G. P. *Anal. Chem.* **1996**, *68*, 3238.

(26) Birks, J. B. *Photophysics of Aromatic Molecules*; Wiley-Interscience: London, 1970.

(27) Kinsel, G. R.; Lindner, J.; Grotemeyer, J.; Schlag, E. W. *J. Phys. Chem.* **1991**, *95*, 7824.

(28) Stemmler, E. A.; Hites, R. A. *Biomed. Environ. Mass Spectrom.* **1987**, *14*, 417.

(29) Born, M.; Ingemann, S.; Nibbering, N. M. M. *Mass Spectrom. Rev.* **1997**, *16*, 181.

(30) Knighton, W. B.; Mock, R. S.; McGrew, D. S.; Grimsrud, E. P. *J. Phys. Chem.* **1994**, *98*, 3770.

(31) Laramée, J. A.; Kocher, C. A.; Deinzer, M. L. *Anal. Chem.* **1992**, *64*, 2316.

(32) Cody, R. M., et al. 46th ASMS Conference on Mass Spectrometry and Allied Topics, June 1998; p 1245.

(33) Data from NIST Webbook and references therein: http://webbook.nist.gov/chemistry/.

(34) In addition, it is conceivable that the accelerating electrons may ionize neutral molecules in the high-density plume generating secondary electrons and positive ions. The source polarity precludes the detection of the complimentary positive ions. The production of negative ions may then proceed through the attachment of these secondary electrons to picric acid.

(35) Chen, E. C. M.; Chen, E. S.; Milligan, M. S.; Wentworth, W. E.; Wiley, J. R. *J. Phys. Chem.* **1992**, *96*, 2385.

(36) Moustefaoui, T.; RebrionRowe, C.; LeGarrec, J. L.; Rowe, B. R.; Mitchell, J. B. A. *Faraday Discuss.* **1998**, *109*, 71.

(37) Canosa, A.; Parent, D. C.; Pasquerault, D.; Gomet, J. C.; Laubé, S.; Rowe, B. R. *Chem. Phys. Lett.* **1994**, *228*, 26.